

Physics 111B: Optical Pumping

Shreyas Patel

Partner: Deanna Long

University of California Berkeley

(Dated: August 8, 2024)

We present an experimental method for determining the nuclear spins of atoms. This experiment was run using two different isotopes of Rubidium, Rb-85 and Rb-87. The value for the ambient magnetic field was also determined using the strength of the Zeeman lines seen in the atoms.

I. INTRODUCTION

Quantum states are used to describe various properties of atoms and molecules. These include but are not limited to the motion and spin of electrons and the spin of the nucleus, and define the eigenstate of the atom and its constituents.

Spectroscopy is a method that can be used to measure the difference in energy between atomic quantum states. If an atom is perturbed with a frequency that matches a difference energy level then a resonant transition can be induced.

In this experiment, we are utilizing specifically on optical pumping and optically detected magnetic resonance (ODMR) as methods to prepare the gas and detect the changes in the spin polarization of the gas. This is to verify the ground state structure and measure nuclear spin of Rubidium isotopes and determine the ambient magnetic field.

This experiment utilizes and applies ideas from quantum mechanics and electromagnetism, such as quantum numbers, spin, fine structure, spin polarization, conservation of angular momentum, selection rules for atomic energy transitions, and magnetic dipole energy.

II. BACKGROUND

A. Atomic Structure

Rubidium (Rb) is an alkali-metal atom with an atomic number of 37. It has two isotopes, Rb-85 and Rb-87, where Rb-85 is the more abundant.

In the ground state, Rb has 1 valence electron in the 5s orbital and the first excited state, the 5p orbital, is 1.6 eV higher in energy. This means that a photon has to be of this energy to create an energy transition, so it would have a wavelength of 820 nm which is in the near-infrared.

Rb atoms exhibit three forms of angular momentum: electron orbital angular momentum (L), electron spin (S), and nuclear spin (I). In the ground state, $L = 0$, $S = 1/2$, but I varies depending on the isotope. For Rb-85 it is $5/2$ and for Rb-87 it is $3/2$. In the excited state, $L = 1$, $S = 1/2$, while I remains the same for the respective isotopes.

Energy levels in the atom are affected by angular momentum. The first-order correction, or splitting, is the fine energy splitting and this is caused by the relativistic effects coupling the L and S quantum numbers. This splits the 5p orbital into the $2P_{1/2}$ and $2P_{3/2}$, but no splitting in the 5s state.

The fine structure splitting is approximately 0.04 eV and affects the optical spectrum of Rb. The transition from ground state to $2P_{1/2}$ occurs at 795 nm (D1 line) and transitions to $2P_{3/2}$ occurs at 780 nm (D2 line).

The next-order splitting is the hyperfine structure caused by the interaction between the L and I quantum numbers. The hyperfine structure is much smaller than the fine structure splitting due to the significant difference in magnetic moments between electrons and nuclei.

In the absence of a magnetic field, the atom's energy eigenstates must also be eigenstates of total angular momentum ($F = I + J$). Ground and excited terms split into states with distinct F values.

B. The Breit-Rabi Formula

The ground state of Rb-87 as an example, it contains 8 distinct quantum states based on different combinations of the $J, I, m_J, \text{ and } m_I$ quantum numbers and are labeled as $|J, I; m_J, m_I\rangle$ and constitute a separable basis.

Another basis choice is a couple basis where states are specified by the total angular momentum F and its projection F_z .

The energy eigenstates and eigenvalues of the atom are described by the hyperfine Hamiltonian H_{hfs} which is defined as:

$$H_{hfs} = -\mu_I \cdot (B_J + B_{ext}) - \mu_J \cdot B_{ext} \quad (1)$$

Here μ_J and μ_I are the magnetic dipole moments of the electrons and nucleus respectively and are defined as such.

$$\mu_J = g_J \mu_B J \quad (2)$$

where

$$\mu_B = \frac{e\hbar}{2m_e} \quad (3)$$

and

$$\mu_I = g_I \mu_N I \quad (4)$$

where

$$\mu_N = \frac{e\hbar}{2m_p} \quad (5)$$

In the equations for μ_B and μ_N , m_e and m_p are the mass of an electron and proton respectively.

Expanding Equation 1, we see that we can get the term $\mu_I \cdot B_J = AhI \cdot J$ which describes the coupling between nuclear and electronic angular momenta and $-(\mu_I + \mu_J) \cdot B_{ext}$ which describes the energies of the atomic magnetic dipoles placed within an externally applied magnetic field.

We can then see that expression for the energy splitting between neighboring Zeeman states to be

$$\frac{\nu}{B_{ext}} = \frac{2.799}{2I+1} \frac{MHz}{G} \quad (6)$$

C. Optical Pumping and Optically Detected Magnetic Resonance

Continuing with Rb-87 as the example, both the separable basis and coupled basis that can be chosen from, they both consist of 8 distinct quantum states for different electronic and nuclear spin orientations.

Optical pumping is a method used to generate spin polarization in atoms. When atoms are exposed to the circularly polarized infrared light, they absorb photons and change their magnetic quantum numbers by m_F by +1. When the electron undergoes spontaneous emission to return to the ground state, it may or may not remain in the higher m_F state. If an electron is already in the highest possible m_F state, it cannot absorb anymore photons since there is no longer a higher state for it to transition into, therefore eventually all of the electrons will get pumped to the highest m_F state, such as $|F=2, mF=2\rangle$ in Rb-87.

The highest-energy hyperfine state depends on the direction of the external magnetic field B_{eff} . If B_{eff} points along the z direction, then $|F=2, mF=2\rangle$ is the highest-energy state. However, if the magnetic field reverses (pointing in the -z direction), the lowest-energy state among the $F=2$ states becomes the final state for optical pumping.

In this experiment, the pumped state achieved through optical pumping is also a dark state since the atom no longer absorbs the light used for optical pumping. This unique feature enables the detection of radio-frequency magnetic transitions within the atomic vapor using optical methods. This technique is known as "optically detected magnetic resonance" (ODMR).

This creates our cycle for how our experiment is run: Without a resonant radio-frequency magnetic field, all atoms are optically pumped into the dark state, causing them to no longer absorb optical pumping light. As a result, a photo-detector measuring light transmitted through the atomic vapor will register a high light level. When a resonant radio-frequency magnetic field is applied, it drives atoms out of the optically pumped state, leads to the absorption of some optical pumping light by the atomic vapor and resulting in a lower light level detected by the photo-detector.

III. EXPERIMENTATION

A. Setup

1. Rb Lamp

The Rb lamp is set up in the center of the two Helmholtz coils that will generate the magnetic field. The lamp itself has a photo-detector on one side, radio frequency oscillator opposite it, and the Rb vapor cell between them. The rf oscillator generates infrared light which passes through a circular polarizer before it reaches the Rb and finally the photo-detector. The polarizer only allows light with a wavelength near 795nm through so that the only electron transitions that occur are D1. There is another coil wrapped around the Rb vapor cell that is connected to the SRS DS345 function generator to generate the radio-frequency magnetic field. A heating coil is also present inside to help prepare the Rb vapor cell by heating it to 50°C so enough Rb is present in the vapor for the experiment.

2. Measurement Instruments

The signal from the photo-detector passes through an amplifier before it reaches the oscilloscope. This signal is wired to the y-axis. The x-axis of the oscilloscope is wired to two different inputs during the course of the experiment. The input is connected to the SRS DS345 while performing a frequency sweep to find the Zeeman resonance for RB-85 and Rb-87. The input is connected to the phase output from the AC modulation unit when trying to find the magnetic resonance. The AC modulation unit modulates the current from the DC power supply that is headed to the Helmholtz coils, creating the variation in the strength of the magnetic field necessary to find the resonance.

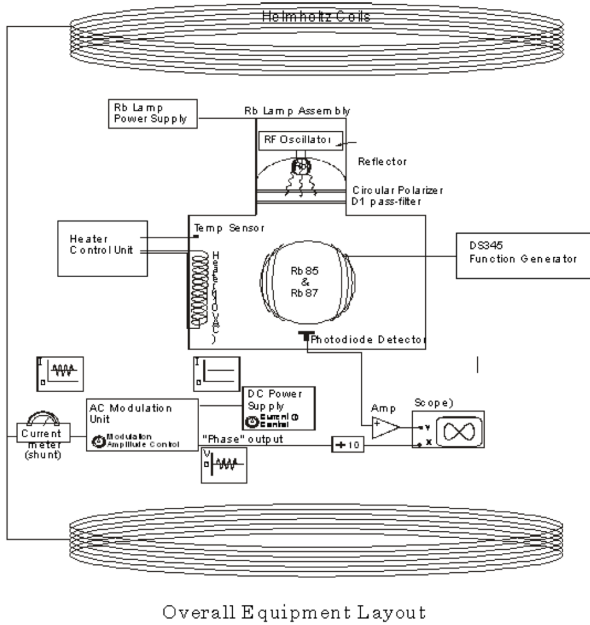


FIG. 1. Diagram of the layout of all the equipment.

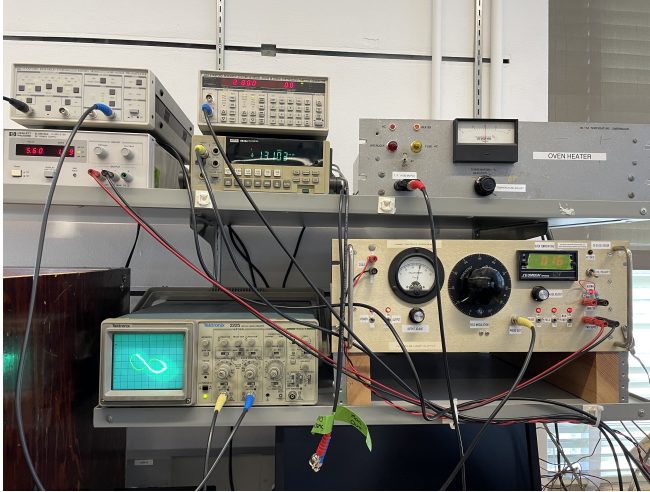


FIG. 2. Picture of the equipment layout in person.

B. Procedure

1. Fixed Current, Sweeping Frequency

For the initial observation of ODMR, the current through the Helmholtz coils was fixed so that way the applied magnetic field would be constant. In these conditions we performed a sweep of the radio frequency using the SRS DS345. During the sweep, the oscilloscope shows two peaks in the photo-detector signal. The two peaks correspond to the resonant frequencies of Rb-85 and Rb-87. The infrared light pumps up the Rb so that way they would become transparent and all the light emitted from

the source hits the photo-detector. If the Rb is exposed to a resonant radio frequency however, this would lower the ground state of the electrons and allow them to be pumped up again, making the gas more opaque. This is what causes the two peaks, one for when each of the Rb isotopes is exposed to their resonant frequency and becomes opaque. The assembly was heated to around 50 °C, the DC current was set to supply 1 A, and set the SRS DS345 to linearly sweep across a 3 MHz range with a 100 ms sweep period.

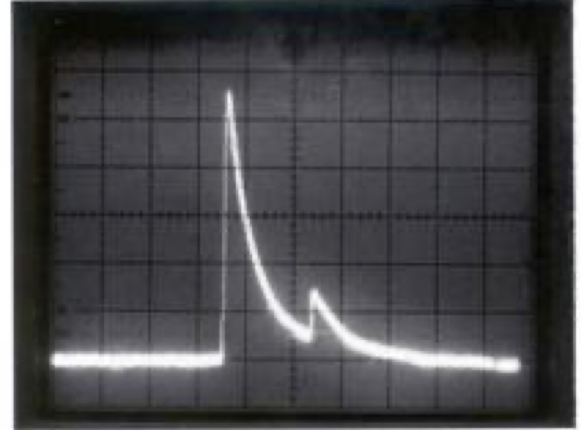


FIG. 3. Example of the rf sweep with the two peaks for the different isotopes.

2. Finding a Good Bulb Temperature

The lamp assembly was heated to a temperature of 54.5 °C and the height of the two peaks was recorded as it cooled. The measurements were initially taken a minute apart, but as the assembly begin to cool slower and slower the time interval between measurements grew since not a significant change would appear in just a minute. The temperature of the assembly is important since enough Rb needs to be present in the vapor to get a stronger measurements. Its good to find a temperature with a decent amount of Rb in the vapor that is also not too high or else it will cool quickly and need to be reheated again. The temperature we found to work well was between 45 °C - 50 °C.

3. Lock-In Detection of Resonance Frequency

One method of finding the resonance frequency is by setting it to be constant and slowly changing the current of the Helmholtz coil until the signal from the photo-detector is at its lowest and that will be our resonance condition. That method is slow so a faster alternative is to modulate the current to the Helmholtz coil and as

a result vary the magnetic field. The x-axis input of the oscilloscope is connected to the phase output of the AD modulation unit. When the resonance condition becomes within range of the modulation, a lemniscate will appear on the oscilloscope screen. When the center of the current modulation corresponds with the resonance condition, then the lemniscate will appear to be symmetrical.

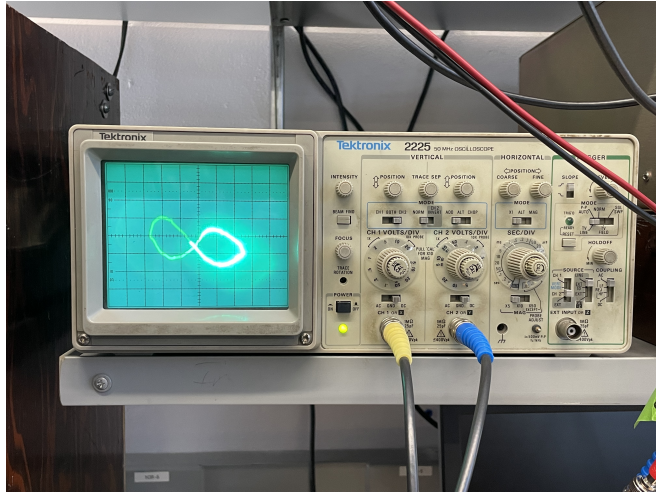


FIG. 4. Example of the resonance figure we are looking for.

This method is much faster since a wide range of current does not need to be tested and instead we can more quickly change the current and look for a more visually apparent criteria. From here, we increase the rf in 0.1 MHz increments and recorded the current for the new resonance. This was repeated again but with decreasing the rf below the initial one. We did have some issues here since the DC power supply we used did not like to go below 1.0 A and became increasingly unstable the lower it went, so measurements corresponding with these current values were harder to do. This measurement was done for both isotopes of Rb and the voltage across the shunt was also recorded for all instances. The direction of current through the coils was then reversed and once again recorded the frequency and current that caused a resonance. We noticed, however, that with negative current no matter what the resonance frequency was set to, the resonance would always only appear when the current through the coils was -0.06 A and voltage across the shunt was around -0.7 mV. This was verified with another DC power supply and we got the same results.

4. Ambient Magnetic Field

We used two procedure to find the ambient magnetic field present in the laboratory. The first method involved setting the current through the Helmholtz coil to zero and finding the Zeeman resonant frequency. We found this by starting at a low rf and using small increments to increase

the rf till we found a resonance structure. We slowly modified the rf, increasing and decreasing in smaller and smaller increments, until we found a symmetrical lemniscate. This would appear when the rf-field was resonant with the ambient magnetic field. The second method did the opposite. The rf-field was turned off and the current through the Helmholtz coils was modulated. Once again, the current was changed until the resonant criteria was found, and this would happen when the magnetic field from the Helmholtz coils was equal and opposite, and therefore cancelled out, the ambient magnetic field.

5. Timescales for Optical Pumping

The rf generator was set to produce a signal with a modulated amplitude. The modulation was done by a square wave that would basically turn the rf generator signal on/off. When the signal was off, the gas will become pumped and the transparent. When the signal was on, the electrons would be "reset" and the gas would become opaque. The "pumping time" and "relaxation time" was recorded based on how long it took for the photo-detector signal to reach a new steady state after a switch in the state of the rf signal. This measurement was done by changing the view of the oscilloscope to show the entirety of both transitions. The number of division was then recorded and multiplied by what the time/div dial was set to on the oscilloscope.

IV. RESULTS & ANALYSIS

A. Data and Results

1. Fixed Current, Sweeping Frequency

The ODMR signals had two peaks, one much larger than the other. The size of the signals is related to the relative abundance of that isotope in the gas, and since Rb-85 is the more abundant isotope, the first peak is associated with that since it is the largest.

2. Finding a Good Bulb Temperature

On average, the peak of the ODRM signals went down as the temperature of the assembly decreases. This was more apparent in the signal for Rb-87 than for Rb-85.

3. Lock-In Detection of Resonance Frequency

Image 4 shows an example of a resonance figure we found.

TABLE I. Measurement of the peak response from the photo-detector while doing a frequency sweep at various temperatures for the inside of the lamp assembly. The measured value for the photo-detector response was the number ticks the peak was above the baseline in the oscilloscope.

Temperature (°C)	Rb-85	Rb-87
54.5	5.0	9.0
52.4	7.0	8.0
51.6	7.0	9.0
50.3	8.5	7.3
49.3	8.0	7.8
48.3	7.5	5.5
47.8	7.0	5.0
47.4	7.5	3.5
46.2	6.5	2.5
45.9	6.3	2.0
45.0	6.0	1.2

TABLE II. Measurement of the current through the Helmholtz coil and voltage across the shunt to get resonance at each radio frequency. The first half of the table was for Rb-85 isotope while the second half was for Rb-87.

Isotope	Frequency (MHz)	Current (A)	Shunt Voltage (mV)
Rb-85	3.3	1.53	15.562
	3.2	1.48	15.067
	3.1	1.43	14.574
	3.0	1.39	14.083
	2.9	1.34	13.59
	2.8	1.29	13.103
	2.7	1.24	12.616
	2.6	1.19	12.124
	2.5	1.14	11.631
	2.4	1.09	11.135
	0.03	-0.065	-0.725
	0.04	-0.07	-0.743
	0.1	-0.06	-0.732
Rb-87	4.644	1.44	14.593
	4.544	1.40	14.261
	4.444	1.37	13.929
	4.344	1.34	13.603
	4.244	1.31	13.269
	4.144	1.27	12.94
	4.044	1.24	12.61
	3.944	1.21	12.28
	3.844	1.175	11.953
	3.744	1.14	11.626
	0.534	-0.065	-0.732
	4.834	-0.065	-0.734
	0.434	-0.065	-0.734

TABLE III. The radio frequency, current through the Helmholtz coil, and voltage across shunt when finding the resonance caused by the ambient magnetic field. The first row is for what radio frequency caused resonance when the only magnetic field present is the ambient one. The second row is for resonance caused by the Helmholtz field canceling the ambient field, with the radio frequency turned off. Both measurements are for measuring the ambient magnetic field.

Frequency (MHz)	Current (A)	Shunt Voltage (mV)
0.249	0.0	-0.007
0.0	-0.07	-0.755

4. Ambient Magnetic Field

Table III shows all of the data we recorded when experimentally determining the magnetic field.

5. Timescales for Optical Pumping

The frequency of the modulating square wave was set to 0.2 Hz. From our observations of the oscilloscope, the "pumping time" of the non-pumped gas lasted from tick -24 to -5 on the x-axis for a total of 19 divisions, while the "relaxation time" lasted from tick 13 to 36 for a total of 13 divisions. The time-trace of the oscilloscope was set to a rate of 0.04 s/div. Whenever the modulation wave turned on or off there would a large spike in the time trace to reflect the sudden change. The measurements were then taken to by seeing how many divisions on the oscilloscope it took for it to return to equilibrium.

B. Analysis

1. Plotting Frequency v Current

Figures 5 - 8 are all graphs the data points collected for the frequency and the current through the Helmholtz coils. The relationship between the two is best fit by a linear model. The model itself is very accurate for the positive current polarity measurements because the χ^2 values for this model were very small. For the negative polarity this was not true. We had a weird behavior where the Helmholtz current that produced resonance for any given frequency was relatively the same. For example, for the Rb-87 isotope the current was the same for all frequencies.

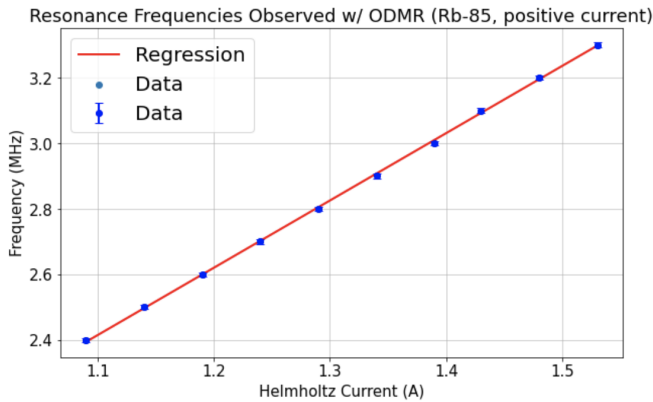


FIG. 5. Frequency vs. Helmholtz current for Rb-85 atom with positive current polarity.

The relationship between frequency and current is best modeled by a linear relationship.

Table IV shows the data for the analysis of the frequency vs. Helmholtz current. There was weird results

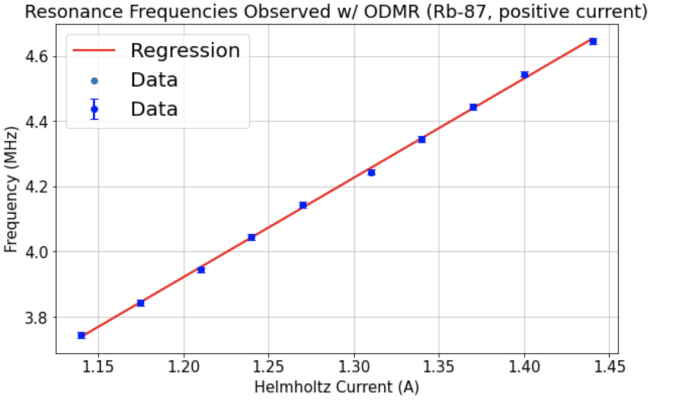


FIG. 6. Frequency vs. Helmholtz current for Rb-87 atom with positive current polarity.

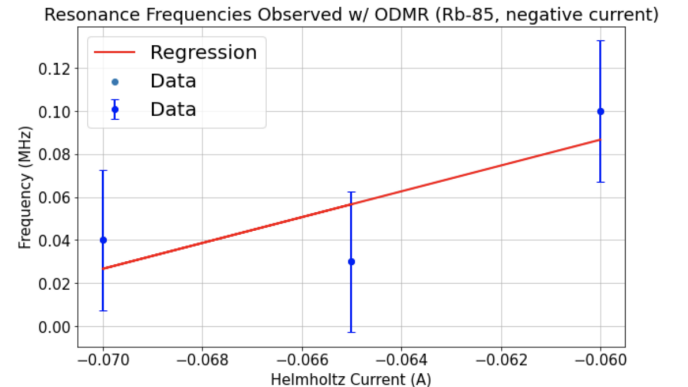


FIG. 7. Frequency vs. Helmholtz current for Rb-85 atom with negative current polarity.

when the polarity of the current was negative where the current did not change. It hovered around -0.065 A at for all frequencies and still produced a resonance figure in the oscilloscope.

2. ν_{85}/ν_{87} Ratio

We cannot directly use data we recorded to determine this ratio because the same current was not used for measurements between the two isotopes. Therefore, we have to use the equation for the best fit model of the two isotopes to calculate this. These are:

$$\nu_{85} = (2.0514 \pm 0.0143)i + (0.1581 \pm 0.0189) \quad (7)$$

$$\nu_{87} = (3.0448 \pm 0.0296)i + (0.2677 \pm 0.0383) \quad (8)$$

So for our ratio we get:

$$\frac{\nu_{85}}{\nu_{87}} = \frac{(2.0514 \pm 0.0143)i + (0.1581 \pm 0.0189)}{(3.0448 \pm 0.0296)i + (0.2677 \pm 0.0383)} \quad (9)$$

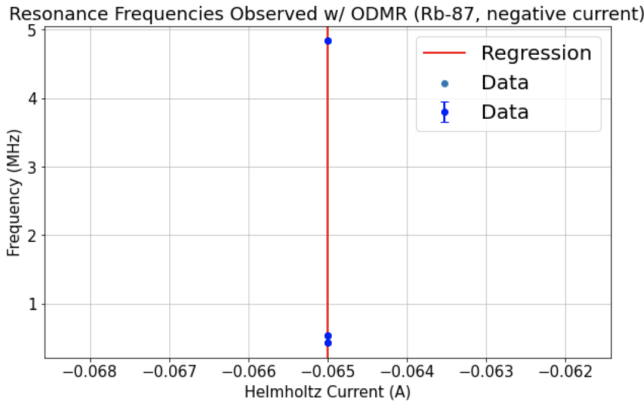


FIG. 8. Frequency vs. Helmholtz current for Rb-87 atom with negative current polarity.

The data calculated from this model is shown in Table IVB 2. From this, we find the average value for ν_{85}/ν_{87} to be 0.6660 ± 0.0277 .

Ratios of ν_{85}/ν_{87} Calculated from Best-Fit Model

Current	Ratio
0.5	0.6578 ± 0.0221
1.0	0.6651 ± 0.0121
1.5	0.6678 ± 0.0083
2.0	0.6692 ± 0.0063
2.5	0.6701 ± 0.0051

3. Calculating Atomic Spin and Ambient Magnetic Field

The magnetic field from the Helmholtz coil is not the only one that is present. An additional ambient magnetic field is necessary to be accounted for resulting in the total external magnetic field being:

$$B_{ext} = B_{coil} + B_{amb} \quad (10)$$

Knowing the magnetic field in the coils to be

$$B_{coil} = (0.9 \times 10^{-2}) \frac{Ni}{a} \quad (11)$$

we can simply the total external field to be

$$B_{ext} = (0.9 \times 10^{-2}) \frac{Ni}{a} + B_{amb} \quad (12)$$

Plugging this into the Breit-Rabi formula and solving for the frequency to better match the model of our graphs, we end up with the equation

$$\nu = \frac{2.799}{2I+1} ((0.9 \times 10^{-2}) \frac{Ni}{a} + B_{amb}) \quad (13)$$

This equation shows the linear relationship between the frequency and the current applied to the Helmholtz coils. For the device used in our lab, $N = 135$ turns and a

$= 0.275$ m. Plugging in these values and further reducing the formula we end up with:

$$\nu = \frac{2.799}{2I+1} (4.418i + B_{amb}) \quad (14)$$

This formula can be looked at as in slope-intercept form, and using the experimentally derived values for the slope and intercepts for the two different isotopes, we can solve for I and then find B_{amb} . Looking at Rb-85 first,

$$\frac{2.799}{2I_{85}+1} 4.418 = 2.0514 \pm 0.0143 \quad (15)$$

$$\frac{2.799}{2I_{85}+1} B_{amb} = 0.1585 \pm 0.0189 \quad (16)$$

Solving for the atomic spin we get that $I_{85} = 2.514 \pm 0.018$. Plugging this into Equation 16 we get that $B_{amb} = 0.3413 \pm 0.0409G$

Repeating the same process for Rb-87 using,

$$\frac{2.799}{2I_{87}+1} 4.418 = 3.0448 \pm 0.0296 \quad (17)$$

$$\frac{2.799}{2I_{87}+1} B_{amb} = 0.2677 \pm 0.0383 \quad (18)$$

we get that $I_{87} = 1.531 \pm 0.015$ and $B_{amb} = 0.3885 \pm 0.0489G$. The B_{amb} calculated from both of these fall within range of each other when the error is accounted for. The actual values of I_{85} and I_{87} are $\frac{5}{2}$ and $\frac{3}{2}$ respectively. The theoretical atomic spin for Rb-85 falls range of the error of the experimentally determined value but the atomic spin for Rb-87 is a bit higher with a percent error of about 2.1Solving for the ratio ν_{85}/ν_{87} , we get

$$\frac{\nu_{85}}{\nu_{87}} = \frac{2I_{87}+1}{2I_{85}+1} = \frac{2(1.531 \pm 0.015) + 1}{2(2.514 \pm 0.018) + 1} = 0.6739 \pm 0.0082 \quad (19)$$

This is within error of the value we calculated for the ratio using purely the best-fit model equations. These calculations were determined using purely the data from the positive polarity current readings. The data from the negative current readings were not included because they did not make physical sense, since a slope of -inf implies an atomic spin of near 0.

4. Other Approaches for B_{amb}

One other approach we can use to find B_{amb} is to measure the resonance frequency for when the current is set to 0 as another way to determine the magnetic field since $B_{ext} = B_{amb}$ in this situation. Our equation then becomes:

$$\nu = \frac{2.799}{2I+1} B_{amb} \Rightarrow B_{amb} = \frac{(2I+1)\nu}{2.799} \quad (20)$$

The resonance frequency for no current was found to be 0.249 MHz as seen in Table III. Since which of the two isotopes this is resonating with is uncertain, it is best to calculate the B_{amb} for both isotopes and calculate the average of the two. Using the I_{85} and I_{87} we calculated from the previous part, our results are:

$$B_{amb,85} = 0.5363 \pm 0.0038G \quad (21)$$

$$B_{amb,87} = 0.3614 \pm 0.0035G \quad (22)$$

Taking the average of these values, we get that $B_{amb} = 0.4489 \pm 0.0052$. This is higher than the ambient magnetic field that was calculated from the previous section using the intercept of the best fit model, but is still within an order of magnitude of that calculation.

One other method for calculating B_{amb} is to find where the magnetic field of the Helmholtz coil cancels the ambient magnetic field. This is because the different spectral lines from the different spin states still exist so the gas can still be pumped in a zero magnetic field, but since the lines are not being spread by an external magnetic field, the corresponding resonance frequency would be zero. Therefore, we would set the frequency to zero and

change the current till a resonance figure is found on the oscilloscope. These measurements are recorded in Table III. Using the current recorded and Equation 11, we find:

$$B_{amb} = 0.3093G \quad (23)$$

This is much closer to the ambient magnetic field that was calculated using the best-fit model in comparison to the value calculated using 0 A current resonance.

V. CONCLUSION

We found that we could experimentally determine the nuclear angular momentum of an atom and where very close to the actual known values. One issue that we ran into with the equipment that effected our readings and measurements was the stability of our DC power supply at negative and very low voltages, making it so we could only rely on positive current measurements for the analysis. The ambient magnetic field also had some discrepancies because of this, but two of our other calculations for this value ended up being fairly close to one another. Ideally, we would swap out our power supply if we were to run this experiment again.

TABLE IV. Data analysis of best fit model and χ^2 data.

Isotope	Current polarity	χ^2	DoF	P-value	σ	$m \pm \sigma_m$	$b \pm \sigma_b$
Rb-85	+	0.0190	8	1.00	0.0063	2.0514 ± 0.0143	0.1585 ± 0.0189
Rb-87	+	0.0369	8	1.00	0.0088	3.0448 ± 0.0296	0.2677 ± 0.0383
Rb-85	-	0.1172	1	0.732099	0.0445	0.2798 ± 0.4183	0.0506 ± 0.0272
Rb-87	-	undef.	1	undef.	undef.	$-\infty$	undef.